Stiffness and Efficiency Optimization of a Hydrostatic Laser Surface Textured Gas Seal

Y. Feldman

Y. Kligerman[1]
Mem. ASME
e-mail: mermdyk@tx.technion.ac.il

I. Etsion
Fellow ASME

Faculty of Mechanical Engineering,
Technion—Israel Institute of Technology,
Technion City,
Haifa 32000, Israel

Microdimples generated by laser surface texturing (LST) can be used to enhance performance in hydrostatic gas-lubricated mechanical seals. This is achieved by applying microdimples with high area density over a certain portion of the sealing dam width adjacent to the high-pressure side, leaving the remaining portion untextured. The textured portion provides an equivalent larger gap that results in converging clearance in the direction of pressure drop and hence, hydrostatic pressure buildup, similar to that of a radial step seal. A mathematical model based on the solution of the Reynolds equation for compressible Newtonian fluid in a narrow gap between two nominally parallel stationary surfaces is developed. A detailed dimensionless analysis of the texturing parameters is performed to achieve maximum gas film stiffness with minimum gas leakage.
[DOI: 10.1115/1.2540120]

Keywords: hydrostatic seal, film stiffness, laser surface texturing, design efficiency parameter

1 Introduction

One main objective in noncontacting mechanical seals is to provide minimal leakage and friction losses during operation. This may be achieved by a small clearance between the mating faces that is just enough to avoid any rubbing contact and allowing some tolerable leakage. Since mechanical seals can experience undesirable vibrations, and since a proper positive stiffness of the lubricant film can provide stable steady-state operation, the seal stiffness is of major importance.

The steady state stability of two phase mechanical seals with both parallel and tapered noncontacting faces was studied extensively by Hughes et al. [1,2] regarding load carrying capacity, lubricant leakage, and film stiffness. Two values for film thickness equilibrium were reported. The larger equilibrium film thickness provides positive film stiffness that is required for robust seal operation but with the smaller equilibrium film thickness any small axial perturbation leads to seal collapse. Etsion and Pascovici [3] studied a two-phase hydrostatic mechanical seal with misaligned faces. It was shown that phase change can be detrimental to the angular stiffness resulting in less stable or even unstable seal operation.

Etsion and Lipshitz [4] suggested a simple method to provide hydrostatic face seals with the necessary axial stiffness. By extending the nosepiece of a conventional hydrostatic seal, the authors developed a new seal configuration having superior performance of maximum film stiffness combined with minimum leakage and friction torque.

Several methods to produce axial stiffness in face seals include various stepped and grooved configurations of one or both of the mating faces. Shellef and Johnson [5] optimized a bi-directional radial groove gas seal to minimize leakage and maximize film stiffness. A set of geometrical relationships was found that substantially increases the seal performance in terms of maximum film stiffness for both hydrostatic and hydrodynamic regimes. A similar optimization for a spiral groove gas seal design was presented by Kowalski and Basu [6] both theoretically and experimentally. Contrary to the bi-directional radial groove seal, the spiral groove design has a preferred direction and when operated in reverse direction the seal has lower stiffness and higher leakage levels.

The stiffness optimization described so far was based on macrovariations of the nominal film thickness. Another way to enhance film stiffness is to employ microsurface texturing on one of the mating surfaces. This can be a more cost effective way than actually manufacture a taper, grooves, or steps. A review of various texturing concepts can be found in Ref. [7] suggesting that of all the microsurface texturing methods, the laser surface texturing (LST) is perhaps the most practical one. This is particularly due to the fact that the laser is extremely fast, environment friendly, and provides an excellent control of the microtexturing parameters, thereby allowing realization of optimum designs.

The first model for LST mechanical seals was offered by Etsion and Burshtein in 1996 [8]. Since then a large volume of theoretical and experimental work was published on various aspects of LST liquid seals [9–14]. Partial LST was successfully employed to enhance hydrostatic effects in high-pressure seals [13], and to reduce breakaway torque and blister formation in carbon–graphite mechanical seal faces [14].

Hydrodynamic gas seals can also benefit from LST as was shown theoretically by Kligerman and Etsion [15] and experimentally by McNickle and Etsion [16]. Recently, Feldman et al. [17] developed a theoretical model to study the effect of partial LST on a hydrostatic gas seal. The authors performed a detailed parametric analysis to find the optimum laser texturing parameters for maximum seal efficiency based on load capacity and leakage considerations.

The main goal of this paper is to complement the preceding work, by optimizing the LST gas seal performance in terms of maximum film stiffness, combined with minimum gas leakage.

2 Analytical Model

A schematic of the partial LST hydrostatic seal that was investigated in Ref. [17] is shown in Fig. 1. The textured face portion, confined by an outer seal diameter d_o and a textured diameter d_p, provides an equivalent larger gap than that of the untextured face portion between d_p and the inner seal diameter d_i. The gas flow, induced by the pressure drop from the sealed high-pressure p_o at

[1]Corresponding author.

Contributed by the Tribology Division of ASME for publication in the JOURNAL OF TRIBOLOGY. Manuscript received August 4, 2006; final manuscript received November 18, 2006. Review conducted by Michael M. Khonsari.

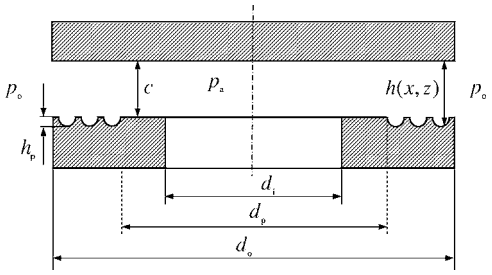

Fig. 1 Schematic of a partial LST mechanical seal

the outer diameter to the ambient pressure p_a at the inner diameter, is therefore in the direction of a converging clearance, leading to hydrostatic pressure buildup.

The mechanical seal in Fig. 1 is characterized by a diameter ratio, d_i/d_o, close to unity (around 0.9) allowing us to neglect the sealing dam curvature and to treat the LST surface as a collection of radial dimple columns. Each column has a length, l, which equals the radial width of the sealing dam and a LST portion length b equal to $(d_o-d_p)/2$. The seal faces are separated by a uniform gas film thickness, c, (see Fig. 1). Periodicity of the surface texturing in the circumferential direction and radial symmetry of each dimple column permit considering the pressure field over only one-half of one dimples column (see Ref. [17]).

The sealed gas is assumed to be compressible and viscous (Newtonian) with a constant viscosity. Dimensionless hydrostatic pressure distribution over just one-half of a single dimple column is obtained from the dimensionless Reynolds equation

$$\frac{\partial}{\partial X}\left(PH^3\frac{\partial P}{\partial X}\right)+\frac{\partial}{\partial Z}\left(PH^3\frac{\partial P}{\partial Z}\right)=0 \tag{1}$$

where the column length l scales the radial x and circumferential z coordinates, the nominal clearance c scales the local film thickness, and p_a scales the pressure field, namely

$$P=\frac{P}{P_a};\quad H=\frac{h}{c};\quad Z=\frac{z}{l};\quad X=\frac{x}{l} \tag{2}$$

Note, that the dimensionless pressure boundary conditions are $P=P_o$ and $P=1$ at $X=0$ and $X=1$, respectively.

The main dimensionless parameters affecting the hydrostatic pressure distribution are: the dimple area density S_p, representing the percentage of textured seal face area between d_o and d_p (see Fig. 1), the dimensionless dimple depth, $\varepsilon=h_p/c$, the dimensionless dimple diameter, $\delta=2r_p/c$, and the textured portion $\gamma=b/l$. The dimple density S_p is assigned a value of 0.65 for high load carrying capacity and to still maintain the validity of the Reynolds equation (see Refs. [17,18]). Each microdimple is located in the center of an imaginary square cell of sides $2r\times 2r$, where $r=r_p\sqrt{\pi/S_p}/2$.

Adopting the approach of Ref. [17], the "equivalent step" height corresponding to the partial LST configuration (see Fig. 2(*b*)) is obtained by dividing the volume of a dimple by the area of its imaginary square cell, hence

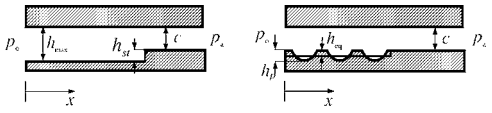

Fig. 2 Schematic of an "equivalent step seal" (*a*); and its corresponding partial LST seal (*b*)

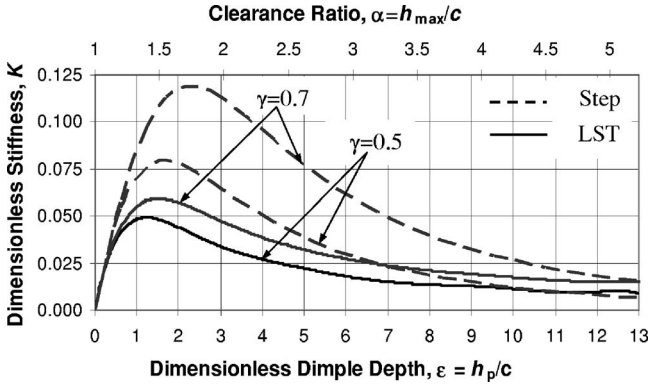

Fig. 3 Dimensionless stiffness, *K*, of the LST and radial step seals versus dimensionless depth ε or corresponding equivalent clearance ratio α, ($P_0=2$, $S_p=0.65$)

$$h_{\text{eq}}=\frac{\pi h_p}{24r^2}(h_p^2+3r_p^2)$$

Thus, the clearance ratio α for an equivalent step configuration (defined by the ratio of maximum film thickness $h_{\max}$ to the nominal clearance c (see Fig. 2(*a*)) is

$$\alpha=\frac{h_{\text{eq}}+c}{c}=\frac{S_p\varepsilon}{6}\left(4\frac{\varepsilon^2}{\delta^2}+3\right)+1$$

Since practical values of the ratio ε/δ are of order 0.1 the first term in the brackets can be neglected yielding the simple relation $\alpha=1+\varepsilon S_p/2$. The analytical expression for the dimensionless average pressure, P_{av}, in the equivalent hydrostatic radial step seal as well as the dimensionless gas leakage, Q, through its boundaries were obtained in Ref. [17].

The seal stiffness k is the derivative of the load carrying capacity with respect to the seal clearance c. In the case of the stepped configuration the clearance ratio α can be expressed as $\alpha=(h_{\text{st}}+c)/c$, where the step depth h_{st} (see Fig. 2(*a*)) is assumed to be constant. Considering the dimensionless definition of the average pressure P_{av} (see Eq. (2)), we have by the chain rule differentiation

$$k_{\text{step}}=-\frac{dp_{\text{av}}}{dc}=-\frac{dp_{\text{av}}}{d\alpha}\frac{d\alpha}{dc}=\frac{P_a}{\text{c}}(\alpha-1)\frac{dP_{\text{av}}}{d\alpha} \tag{3a}$$

It was shown in Ref. [17] that the average pressure P_{av} of a partial LST hydrostatic gas seal is independent of the dimensionless dimple diameter for practical values of $\delta>60$. Thus, the LST seal film stiffness is also independent of δ. Similar to Eq. (3*a*), and using the definition $\varepsilon=h_p/c$, the LST seal film stiffness may be expressed as

$$k_{\text{LST}}=-\frac{dp_{\text{av}}}{dc}=-\frac{dp_{\text{av}}}{d\varepsilon}\frac{d\varepsilon}{dc}=\frac{P_a}{c}\varepsilon\frac{dP_{\text{av}}}{d\varepsilon} \tag{3b}$$

Normalizing the film stiffness, k, in Eqs. (3*a*) and (3*b*) by p_a/c, the dimensionless film stiffness, K, is

$$K=k/(p_a/c) \tag{4}$$

3 Results and Discussions

3.1 Film Stiffness. Figure 3 presents the dimensionless film stiffness, K, of the partial LST seal versus its dimensionless dimple depth ε (solid lines) along with the stiffness of the corresponding equivalent radial step seal versus its clearance ratio α (dashed lines). The results are shown for a typical case with $S_p=0.65$, $P_0=2$ and two optimum values of textured portion (or step location), $\gamma=0.7$ for maximum load carrying capacity P_{av} and γ

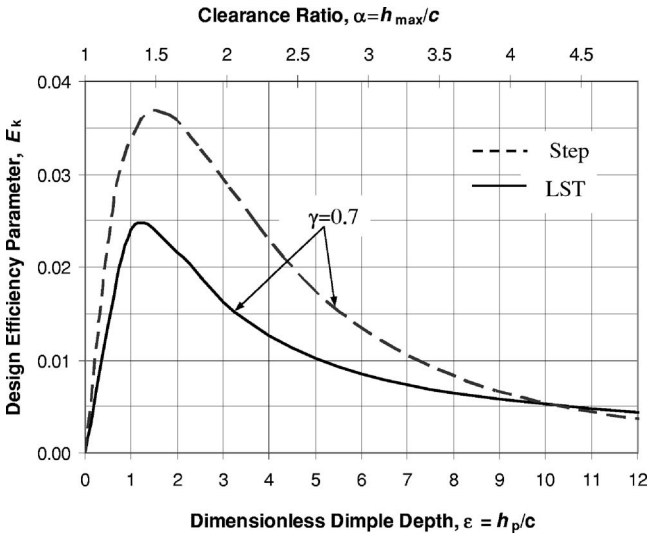

Fig. 4 Design efficiency parameter of the LST or radial step seals versus dimensionless depth ε or corresponding equivalent clearance ratio α, (P_0=2, S_p=0.65)

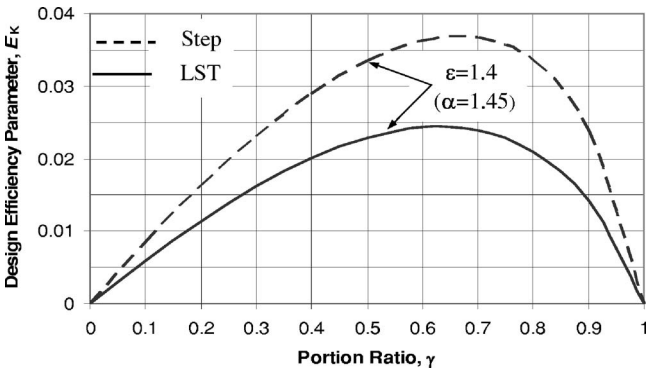

Fig. 5 Design efficiency parameter of the LST and radial step seals versus textured portion (or step location) γ, (P_0=2, S_p=0.65)

=0.5 for maximum P_{av}/Q ratio (see Ref. [17]).

As can be seen from Fig. 3 the maximum film stiffness, K, of the LST seal corresponds to an ε value of about 1.4 for both γ =0.5 and γ=0.7. The equivalent radial step seal is characterized by an optimum α value of about 1.7. As illustrated in Fig. 3, the radial step configuration has a more pronounced maximum K values compared with the LST configuration. The optimum K values of the LST seal are between 50% and 60% of those of the corresponding K values for a stepped configuration. Also, as can be seen from Fig. 3, the variation of K with γ is more pronounced in the stepped configuration.

3.2 Design Efficiency Parameter, E_k. In Ref. [17] an efficient seal design was suggested based on maximizing the ratio P_{av}/Q. It seems more practical to base the efficient design on maximizing the ratio K/Q. This will expand the former optimization from an ideal steady-state case to a real life application involving disturbances of the seal clearance. In this case the efficient design provides a more stable seal operation.

Figure 4 presents the new design efficiency parameter, E_k =K/Q, for a partial LST seal versus its dimensionless depth ε, and for an equivalent radial step seal versus its corresponding values of clearance ratio α. The results are presented for γ=0.7, which yields maximum K value for the partial LST seal (see Fig. 3). As can be seen the LST configuration has an optimum value ε=1.4 for a maximum design efficiency parameter, E_k, and the optimum stepped seal corresponds to α=1.5. These optimums are sharp and even moderate deviations (no more than ±0.5) from them result in up to 30% decrease for the LST seal, and up to 20% decrease for the radial step seal in the design efficiency parameter.

The effect of the textured portion (or step location) γ on the design efficiency parameter, E_k, for both LST and equivalent radial step configurations is presented in Fig. 5. The plots are given for the optimum dimensionless dimple depth ε=1.4 (or α=1.45) that maximizes the LST efficiency parameter E_k (see Fig. 4). As shown in Fig. 5, the optimum design corresponds to a textured portion (or step location) value of γ=0.65. In addition, the maximum E_k value of the partial LST seal comprises about 66% of the corresponding maximum E_k value of the equivalent radial step seal. This optimum is relatively shallow, leading to insignificant (no more then 10%) variations in the efficiency parameter values while γ deviates by ±0.1 from its optimal value.

LST is much simpler and cost effective compared to conventional machining techniques. Hence, considering it is almost as efficient as the equivalent step, the LST seems an attractive alternative in enhancing hydrostatic gas seals performance.

4 Conclusion

The potential of partial laser surface texturing for enhanced robust steady-state operation of hydrostatic gas seals was investigated numerically. A detailed parametric analysis was performed to optimize laser texturing parameters in terms of maximum film stiffness and design efficiency parameter. A textured portion value of γ=0.7 and dimensionless dimple depth value of ε=1.4 provide maximum film stiffness and design efficiency parameters over a wide range of LST parameters and operating conditions.

Nomenclature

b = LST portion length
c = clearance
d_i = inner seal diameter
d_o = outer seal diameter
d_p = textured diameter
E_k = design efficiency parameter, $E_k=K/Q$
h_p = dimple depth
h = local film thickness inside the imaginary cell
h_{st} = step depth
H = dimensionless film thickness, $H=h/c$
k = seal stiffness
k_{LST} = LST seal film stiffness
k_{step} = radial step seal film stiffness
K = dimensionless seal stiffness, $K=k/(p_a/c)$
l = radial dimple column length
p_a = ambient pressure
p_o = high pressure
p_{av} = average pressure
P = dimensionless pressure, $P=p/p_a$
Q = dimensionless gas leakage
r = imaginary cell half length
r_p = dimple radius
S_p = dimple density
x, y, z = Cartesian coordinates
X, Z = dimensionless coordinates, $X=x/l$, $Z=z/l$
α = equivalent radial step seal clearance ratio, $\alpha=h_{max}/c$
γ = textured portion, $\gamma=b/l$
δ = dimensionless dimple diameter, $\delta=2r_p/c$
ε = dimensionless dimple depth, $\varepsilon=h_p/c$

References

[1] Hughes, W. F., Winowich, N. S., Birchack, M. J., and Kennedy, W. C., 1978, "Phase Change in Liquid Face Seals," ASME J. Lubr. Technol., **100**, pp. 74–80.

[2] Hughes, W. F., and Chao, N. H., 1980, "Phase Change in Liquid Face Seals II—Isothermal and Adiabatic Bounds with Real Fluids," ASME J. Lubr. Technol., **102**, pp. 350–359.

[3] Etsion, I., and Pascovici, M. D., 1996, "Phase Change in a Misaligned Mechanical Face Seal," ASME J. Tribol., **118**, pp. 109–115.

[4] Lipshitz, A., and Etsion, I., 1978, "A Modified Face Seal for Positive Film Stiffness," ASLE Trans., **21**, pp. 356–360.

[5] Shellef, R. A., and Johnson, R. P., 1992, "A Bi-Directional Gas Face Seal," Tribol. Trans., **35**, pp. 53–58.

[6] Kowalski, C. A., and Basu, P., 1995, "Reverse Rotation Capability of Spiral-Groove Gas Face Seals," Tribol. Trans., **38**, pp. 549–556.

[7] Etsion, I., 2005, "State of the Art in Laser Surface Texturing," ASME J. Tribol., **127**, pp. 248–253.

[8] Etsion, I., and Burstein, L., 1996, "A Model for Mechanical Seals with Regular Microsurface Structure," Tribol. Trans., **39**, pp. 677–683.

[9] Etsion, I., Kligerman, Y., and Halperin, G., 1999, "Analytical and Experimental Investigation of Laser-Textured Mechanical Seal Face," Tribol. Trans., **42**, pp. 511–516.

[10] Etsion, I., 2000, "Improving Tribological Performance of Mechanical Seals by Laser Surface Texturing," *Proceedings of the 17th International Pump Users Symposium*, Houston, TX, March 6–9, pp. 17–22.

[11] Yu, X. Q., He, S., and Cai, R. L., 2002, "Frictional Characteristics of Mechanical Seals with a Laser-Textured Seal Face," J. Mater. Process. Technol., **129**, pp. 463–466.

[12] Hoppermann, A., and Kordt, M., 2002, "Tribological Optimization Using Laser-Structured Contact Surfaces," O+P Oelhydraulik und Pneumatik, **46**(4), Vereinigte Fachverlage Mainz.

[13] Etsion, I., and Halperin, G., 2002, "A Laser Surface Textured Hydrostatic Mechanical Seal," Tribol. Trans., **45**, pp. 430–434.

[14] Pride, S., Folkert, K., Guichelaar, P., and Etsion, I., 2002, "Effect of Micro-Surface Texturing on Breakaway Torque and Blister Formation on Carbon-Graphite Faces in a Mechanical Seal," Lubr. Eng., **58**, pp. 16–21.

[15] Kligerman, Y., and Etsion, I., 2001, "Analysis of the Hydrodynamic Effects in a Surface Textured Circumferential Gas Seal," Tribol. Trans., **44**, pp. 472–478.

[16] McNikel, A., and Etsion, I., 2004, "Near-Contact Laser Surface Textured Dry Gas Seals," ASME J. Tribol., **126**, pp. 788–794.

[17] Feldman, Y., Kligerman, Y., and Etsion, I., 2006, "A Hydrostatic Laser Surface Textured Gas Seal," Tribol. Lett., **22**, pp. 21–28.

[18] Feldman, Y., Kligerman, Y., Etsion, I., and Haber, S., 2006, "The Validity of the Reynolds Equation in Modeling Hydrostatic Effects in Gas Lubricated Textured Parallel Surfaces," ASME J. Tribol., **128**, pp. 345–350.